THE ASEAN JOURNAL OF RADIOLOGY 2013: 19(1): 51-66 51

Original Article

Magnetic Resonance Imaging Features of Intramedullary Spinal Cord Tumors with Pathological Correlations

Jureerat Thammaroj, MD
Amnat Kitkhandee, MD
Parinyaporn Tumkot, MD
Pichayen Duangtongpol, MD
Sakda Waraosawapati, MD

Department of Radiology, Neurosurgery, Pathology
Faculty of Medicine, Khon Kaen University, Khon Kaen, Thailand, 40002

Abstract

Objective: The purpose of this study was to determine characteristic imaging findings of intramedullary spinal cord tumor in magnetic resonance imaging (MRI).

Material and Methods: We retrospectively analyzed MRI in 15 patients with histologicaly proven intramedullary spinal cord tumors. The demographic data, MRI findings with histological findings were recorded in terms of age, location, length, morphology, signal intensity, the presence or absence of cyst and hemorrhage, enhancement pattern, other associated findings, necrosis, vascular proliferation and WHO grading.

Results: Among the 15 patients, spinal cord ependymomas were eccentric 75%, well-define border 62.5% and cervicothoracic spine located 37.5%.

Spinal cord astrocytomas were eccentrically located and ill-define border 85.7%, cervicothoracic and thoracic spine located 28.5%. A cystic component was seen in 87.5% of spinal cord ependymoma and 71.5% of astrocytomas. Intratumoral hemorrhage occurred in 75% of spinal cord ependymomas, and 57.1% of astrocytomas. In 12.5% of spinal cord ependymomas, a curvilinear low T2 signal, suggesting marginal hemorrhage, was seen at the upper and/or lower margins of the tumors. Twenty-five percent of spinal cord ependymoma and 57.2% of astrocytomas showed heterogeneous enhancement, while in 12.5% of spinal cord ependymomas, enhancement was homogeneous.

Conclusion: Although no statistically significant characteristic MRI feature to distinguish between ependymoma and astrocytoma is detected. By percentage we found that border, length and signal intensity of tumors may help diagnosis. With pathological correlation, all of spinal cord ependymomas are mark hypervascular tumor, but astrocytomas never showed.

Introduction

Intramedullary spinal cord tumors account for approximately 25% of spinal tumors. Ependymoma is the most common intramedullary cord tumors, account for about 60%[1]. Whereas astrocytoma for approximately 30%[2]. The differential diagnosis of spinal tumors is primarily based on location, but the clinical presentation, age, and gender of the patient are also important factors in determining the diagnosis[3].

Magnetic resonance imaging (MRI) has been the sensitive tool for detection and diagnosis of intramedullary spinal cord tumors. With its multiplanar capabilities and high contrast resolution, it allows identification and characterization of the lesion as a noninvasive modality. The addition of intravenous contrast administration allows further delineation of the mass, separating tumor from edema and cysts. The exact histologic diagnosis of tumors remains elusive on the basis of MR signal intensity and enhancement alone. However, there are some imaging characteristics which can be suggest the diagnosis[4].

The goals of surgery are to obtain a tissue diagnosis and to improve neurological function by removing the tumor. It is important to identify type of spinal cord tumors, because proper treatment of different subtypes can reduce the rate of disability and functional impairment. Proper preoperative diagnosis is crucial for neurosurgeon, because most ependymoma is well demarcated from cord tissue, can be totally removed and usually result in cure, whereas astrocytoma always infiltrate the surrounding cord tissue, making total resection is impossible[1]. The traditional treatment of intramedullary astrocytoma has been biopsy or debulking followed by radiation therapy[5]. Outcome for intramedullary spinal cord astrocytoma is significantly worse than that of ependymoma and is most closely predicted by pathological grade[6]. The purpose of this study was to determine characteristic imaging findings of intramedullary spinal cord tumor in magnetic resonance imaging (MRI).

Material and methods

We retrospectively analyzed MRIs in 15 patients with intramedullary spinal cord tumors from 1st January 2006 to 31th October 2011 at Srinagarind Hospital, KhonKaen University, Thailand. All patients were treated surgically, and pathological confirmations were obtained.

All MRI studies had been obtained by using a 1.5T scanner (GE; Signa Horizon). The protocol included spin-echo T1 weighted, fast spin-echo T2 weighted images in axial and saggital plane, proton density image in saggital plane and post contrast-enhanced (0.2 mmol per kilograms of body weight) fat suppressed fast spin-echo T1 weighted image in axial and saggital plane. Section thicknesses were about 4 mm. and 5 mm. in sagittal and axial images, respectively.

All of MRI studies and proven histological data were evaluated by a fourteen years experienced radiologist and pathologist by single blind technique. The tumor characteristic were recorded in term of location, length, morphology, signal intensity, the presence or absence of cyst and hemorrhage, enhancement pattern, and other associated findings. Additional the results of histology were assessed with cystic component, intratumoral hemorrhage, necrosis, vascular proliferation and WHO grading.

For each imaging sequences, the signal intensity of spinal tumors was compared with spinal cord. The location of the solid tumors was classified as

central or eccentric on the axial image, eccentric indicating that the whole of tumor was laterally placed. In addition, intramedullary spinal cord tumors were assessed with anatomical location (cervical, thoracic, lumbar, cervicothoracic, thoracolumbar, thracolumbosacrum), longitudinal length (number of vertebral segments involving tumor), T1 and T2 signals relative to the spinal cord (hypointense, isointense, hyperintense, hypo-isointense and hypo-hyperintense).

Peritumoral cyst was defined as a cyst at caudal or rostral to the solid tumors without contrast enhancement of its wall, while an intratumoral cyst was define as a cyst within the tumor with enhancement of its wall(If areas of high signal intensity were obscured at non-enhanced T1-weighted image, intratumoral hemorrhage was thought to be present). The presence or absence of a low signal intensity rim at the boundaries of the tumor at T2-weighted imaging, suggesting marginal hemorrhage, was evaluated. The tumor enhancement patterns were classified into the following categories according to the area of solid tumor enhancement and homogeneity: 1) no enhancement, 2) focal nodular enhancement, 3) patchy enhancement (enhancement of less than one-half of the solid portion of the tumor), 4) heterogeneous enhancement (inhomogeneous enhancement of one-half or more of the solid portion of the tumor), and 5) homogeneous enhancement (homogeneous enhancement of one-half or more of the solid portion of the tumor).

Result

Of 15 patient intramedullary spinal cord tumors, 8 patients were ependymomas and 7 patients were astrocytomas.

Age and Gender

The patient age ranged from 26 to 60 years (mean = 43) of spinal cord ependymoma and 3 to 47 years (mean = 23) of spinal cord astrocytoma, respectively. The demographic data are summarized in Table 1.

Tumor morphology and location

Spinal ependymoma appears eccentric located 6/8 (75%), well-defined border 5/8 (62.5 %), ill-defined border 3/8 (37.5) and central located 2/8 (25%), whereas astrocytoma shows eccentric located 6/7 (85.7%), ill-define border 6/7 (85.7%), well-define border 1/7 (14.3%) and central located 1/7 (14.3%).

Spinal cord ependymoma locate at CT spine 3/8 (37.5 %), lumbar spine 2/8 (25 %), TL spine 1/8 (12.5 %), cervical spine 1/8 (12.5%), and TLS spine 1/8 (12.5%), respectively. Spinal cord astrocytomas locate at CT spine 2/7 (28.5%), thoracic spine 2/7 (28.5%), cervical spine 1/7 (14.3%), lumbar spine 1/7 (14.3%), and TL spine 1/7 (14.3%), respectively. The findings appear in Table 2.

Tumor length

The lesions varied from 2 to 18 vertebral segments (mean = 7.8 vertebral segments) in length along the neuraxis of spinal cord ependymomas and 3 to 8 vertebral segment (mean=5.4 vertebral segments) of spinal cord astrocytomas. The findings appear in Table 2.

Signal Intensity

At TI-weighted imaging, 3/8 (37.5%) spinal cord ependymomas were iso-hyperintense and 3/7 (42.9%) were low-isointense of spinal cord astrocytomas.

At T2-weighted imaging, 6/8 (75%) of spinal cord ependymoma were hyperintense and 4/7

(57.2%) of spinal cord astrocytomas were hyperintense relative to the signal intensity of spinal cord.

Enhancement Pattern

Among the 15 patients who underwent contrast-enhanced scanning, tumor enhancement was demonstrated in all spinal cord tumors. Enhancement pattern was focal nodular in three (37.5%), heterogeneous enhancement in two (25%), patchy enhancement in two (25%) and homogeneous enhancement in one (12.5%) of eight spinal cord ependymomas (Fig 1), while among seven spinal cord astrocytomas, the observed pattern was heterogeneous in 4 (57.2%). In two cases (28.5%) were focal nodular enhancement (Fig 2) and one case (14.3%) was patchy enhancement. The MR imaging findings of spinal ependymomas and astrocytomas are summarized in Tables 2.

Cyst and Hemorrhage

Seven of 8 spinal cord ependymomas (87.5%) had reactive cystic component, both rostral and caudal cysts 3/8 (37.5%), caudal 2/8 (25%) and rostral 1/8 (12.5%) cysts (Fig 3 and 4) and intratumoral cyst 1/8 (12.5%) were present. Among spinal cord astrocytomas had cysts 4/7 (57.2%), cyst type was rostral 1/7 (14.3%), caudal 1/7 (14.3%), syringohydromyelia 1/7 (14.3%) and intratumoral cyst 1/7 (14.3%).

Intratumoral hemorrhage occurred in 6 of 8 (75%) spinal cord ependymoma (Fig 5), while 4 of 7 (57.1%) astrocytomas occurred. At T2-weighted imaging, rim(s) of low signal intensity, suggesting marginal hemorrhage between normal and tumoral tissue, were seen at the upper or lower margins of 1 (12.5%) of 8 spinal cord ependymoma.

Histological findings

Eight spinal ependymomas were tanocytic type 12.5% (1) and myxopapillary type 12.5% (1). All of ependymomas were WHO grade II. Low grade (I-II) spinal cord astrocytomas were 4/7 (57.1%), three were pilocytic astrocytoma grade I (42.8%), one was astrocytoma grade II (14.3%). High grade (III-IV) were 3/7 (42.9%) of spinal astrocytomas, two were anaplastic astroctyma grade III (28.6%) and one was glioblastoma multiforme grade IV (14.3%).

There had intratumoral cysts about four (57.1%) of seven spinal astrocytomas (Fig 6) and three (37.5%) of eight spinal ependymomas. Intratumoral hemorrhage were found six (85.7%) of seven spinal astrocytomas and four (50%) of eight spinal ependymomas. Vascular proliferation found 42.9% of three high grade astrocytomas. Necrosis areas were found one (14.7%) of seven spinal astrocytoma and one (12.5%) of eight spinal ependymoma. All of ependymomas show mark hypervascularity, while two of seven (28.5%) spinal astrocytomas appear moderate hypervascularity. The others associated findings such as true ependymal rosette and/or perivascular rosette found about two (25%) of eight of spinal cord ependymomas. Rosenthal fiber was found three

Table 1. Patient Information

Diagnosis	Age (mean)	Male (%)	Female (%)
Ependymoma	26-60 years (43)	12.5	87.5
Astrocytoma	3-47 years (23)	28.6	71.4

Table 2. Summary of MR Imaging Findings of Spinal Cord tumor

	Ependymoma (n=8)	Astrocytoma (n=7)	p-value
Morphology	37.5 %	14.3 %	0.569
Well-define	62.5 %	85.7 %	
Ill-define			
Axial location	75%	85.7%	>0.999
Eccentric	25%	14.3%	
Central			
Longitudinal location			
Cervical spine	12.5%	14.3%	
Thoracic spine	0%	28.5%	
Lumbar spine	25%	14.3%	0.874
Cervicothoracic spine	37.5%	28.5%	
Thoracolumbar spine	12.5%	14.3%	
Thoracolumbarsacral spine	12.5%	0%	
Length of tumors (mean)	2-18 vertebral segments (mean=7.8)	3-8 vertebral segments (mean=5.4)	
Signal intensity			
T1W			
Isointense	12.5%	28.5%	
Hypointense	25%	28.5%	
Hyperintense	0%	0%	
Iso-hypointense	25%	42.9%	0.483
Iso-hyperintense	37.5%	0%	
T2W			
Isointense			
hypointense			
Hyperintense	75%	57.2%	
Iso-hypointense			0.608
Hypo-hyperintense	25%	42.8%	
Cystic component			
None	12.5%	42.8%	
Rostal	12.5%	14.3%	
Rostal with caudal	37.5%		
Caudal	25%	14.3%	
Syringohydromyelia		14.3%	
Intratumoral cyst	12.5%	14.3%	0.096
Intratumoral hemorrhage	75%	57.1%	
Hemosiderin cap	12.5%	-	
Enhancement pattern			
No enhancement			
Homogeneous	12.5%		
Heterogeneous	25%	57.2%	> 0.999
Focal nodular	37.5%	28.5%	
Patchy enhancement	25%	14.3%	0.720

Table 3. Summary of pathological findings of spinal cord tumor

	Ependymoma (n=8)	Astrocytoma (n=7)
WHO grading	Tanocytic type; 12.5% Myxopapillary type; 12.5% Other type; 75%	Grade I; 42.8% Grade II; 14.3% Grade III; 28.6% Grade IV; 14.3%
Cystic component	37.5%	57.1%
Intratumoral hemorrhage	50%	85.7%
Necrosis	12.5%	14.7%
Vascular proliferation	-	42.8%
Calcification	-	-
Other findings	Mark hypervascularity; 100% True ependymal rosette or perivascular rosette; 25%	Moderate hypervascularity; 28.5% Rosenthal fiber; 42.8%

(42.8%) of seven spinal cord astrocytomas. Neither spinal cord ependymomas nor astrocytoma had intratumoral calcification. The histological findings of spinal ependymomas and astrocytomas are summarized in Tables 3.

Discussion

Ependymomas are the most common spinal cord tumors in adults, with a peak incidence in the fourth and fifth decades, and account for 60% of all intramedullary tumors[3]. Spinal cord astrocytomas are the most commonly occurring intramedullary tumors in children and the second most common spinal cord tumor in adults, age at presentation is 30 years[3,7,8]. Consistent with our series, we found spinal ependymomas occurred between 26 and 60 years (mean age 43 years) where as spinal astrocytomas occurred in the younger age group patient ranged from 26 to 60 years, mean age 23 years.

The majority of ependymomas arise in the cervical spinal cord, with 44% in the cervical cord alone and 23% involving the upper thoracic spinal cord as well[3]. The myxopapillary ependymomas are commonly present in the conus medullaris and the filum terminale[3, 7]. Ependymomas originate from the ependymal walls and as such are more centromedullary located compared with astrocytomas[9]. They are usually well circumscribed and do not infiltrate adjacent cord tissue. Astrocytomas are more frequent in the cervical and the thoracic regions[10]. The typical astrocytoma is large, eccentrically located and frequently ill-defined margin[9]. The mean size of the ependymoma corresponds to a mean height of three to four vertebral bodies (min. 2, max. 13), whereas astrocytomas are usually more extension, with a mean height of 5.6 vertebral bodies (min. 2, max. 19)[9]. In contrast, we found that most of spinal cord ependymomas and astrocytomas were eccentric location, 6/8 (75%) and 6/7 (85.7%), respectively. Spinal cord ependymomas had longer extension than spinal cord astrocytomas, 7.8 and 5.4 vertebral segments, respectively.

Ependymomas commonly are hyperintense on T2WI. Myxopapillary ependymoma is usually hyperintense on T1 because of mucinous content or hemorrhage content[10], whereas most non-myxopapillary

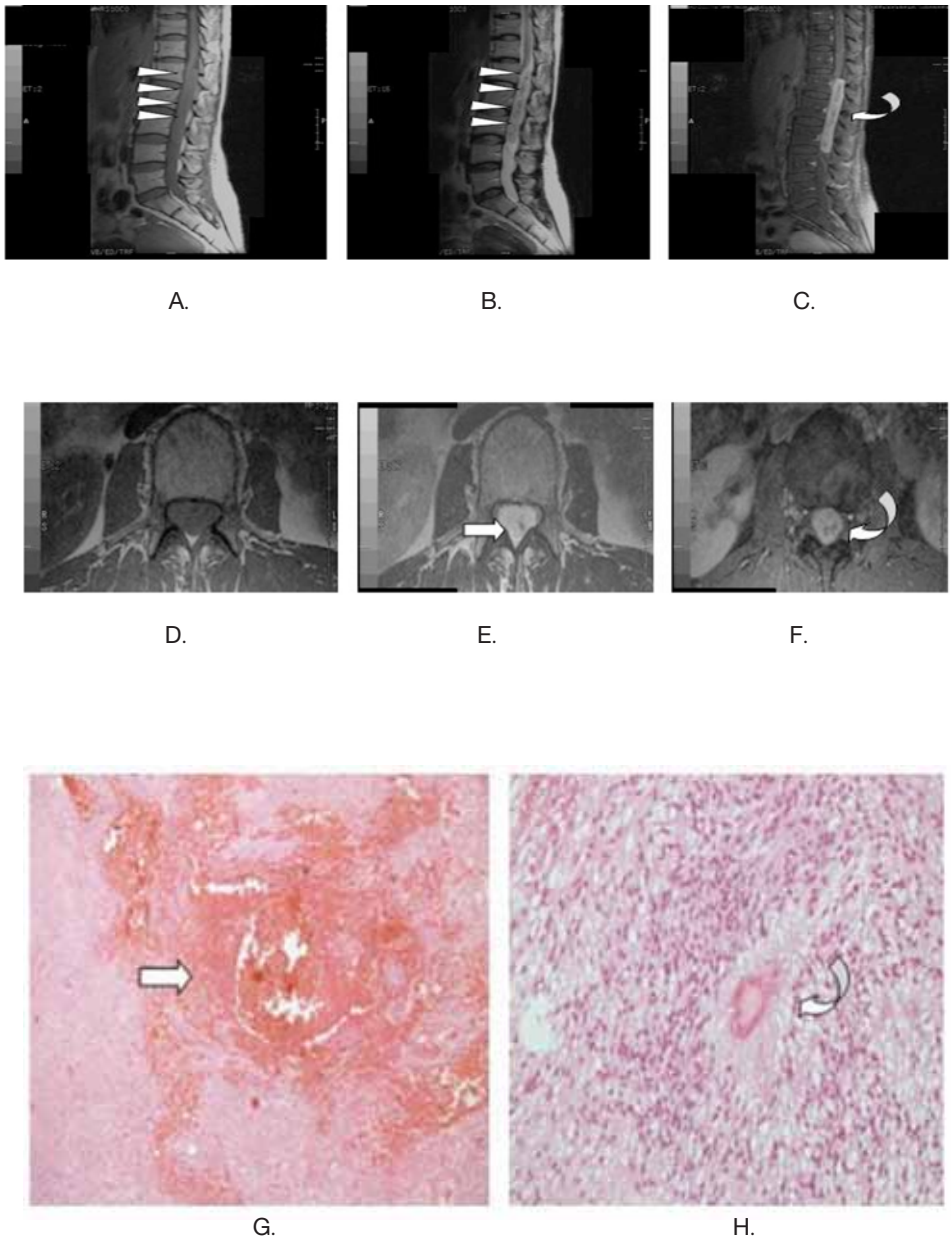

Fig 1 Typical spinal cord ependymoma (WHO grade II) in 49 year-old woman. (A) T1-weight sagittal image show well-define iso SI intramedullary tumor from L1-L4 spine epiconus region and exhibit mix hypo-hyper SI on (B) T2-weight sagittal image (arrow head). (C) Fat suppressed CE T1-weight axial image show intense homogeneous enhancement (curve arrow). (D) T1-weight axial image show small area of iso SI and exhibits low SI area on (E) T2-weight gradient axial image, representing intratumoral hemorrhage (white arrow). (F) Fat suppressed CE T1-weight axial image show intense enhancement. (G) and (H) Histology show area of intratumoral hemorrhage (arrow) and perivascular rosette formation (curve arrow).

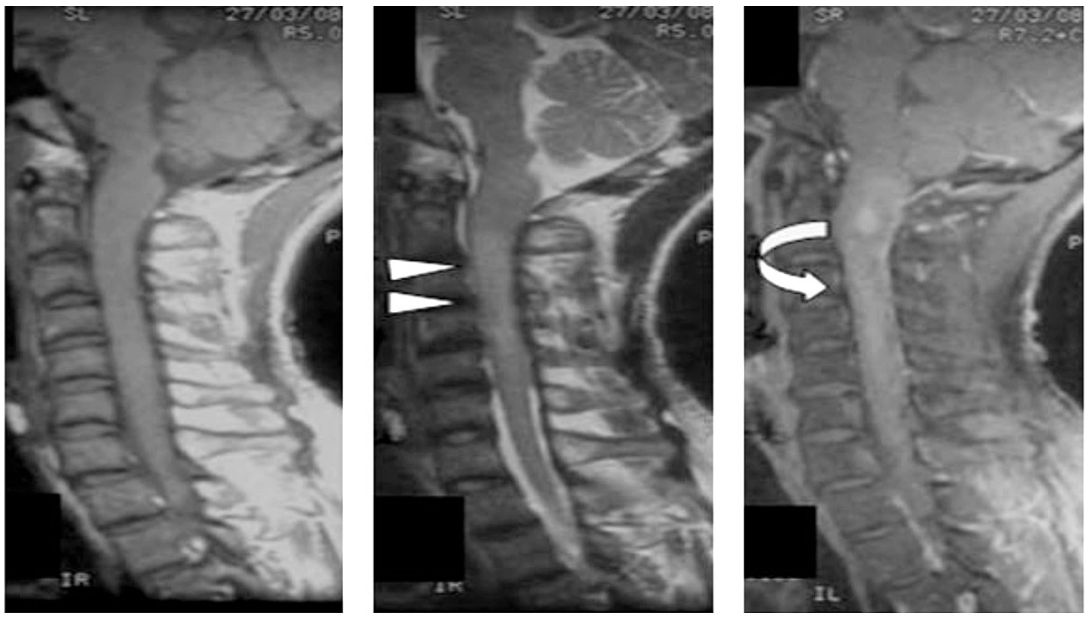

A. B. C.

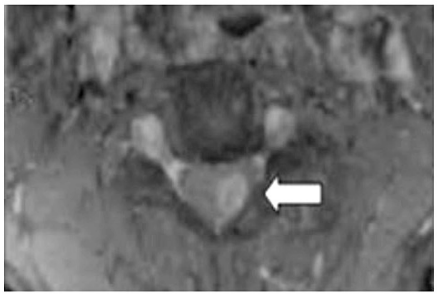

D.

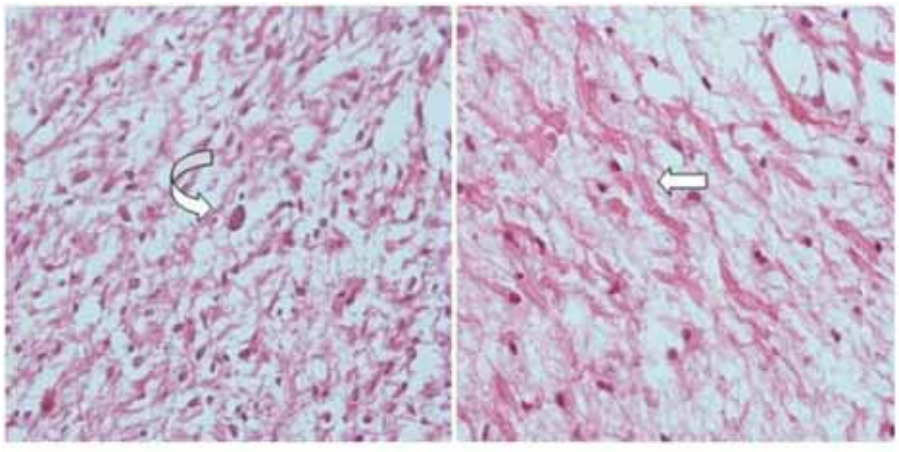

E. F.

Fig 2 Typical spinal cord pilocytic astrocytoma (WHO grade I) in 47 years old woman. (A) T1-weight sagittal image show ill-define iso SI intramedullary spinal cord tumor and exhibit heterogeneous hyper SI on (B) T2-weight sagittal image (arrow head). (C) and (D) Fat suppressed CE T1-weight sagittal and axial image show focal nodular enhancement of tumors (white arrow). (E), (F) and (G) Histology show atypical astrocyte (curve arrow) and rosenthal reaction (arrow).

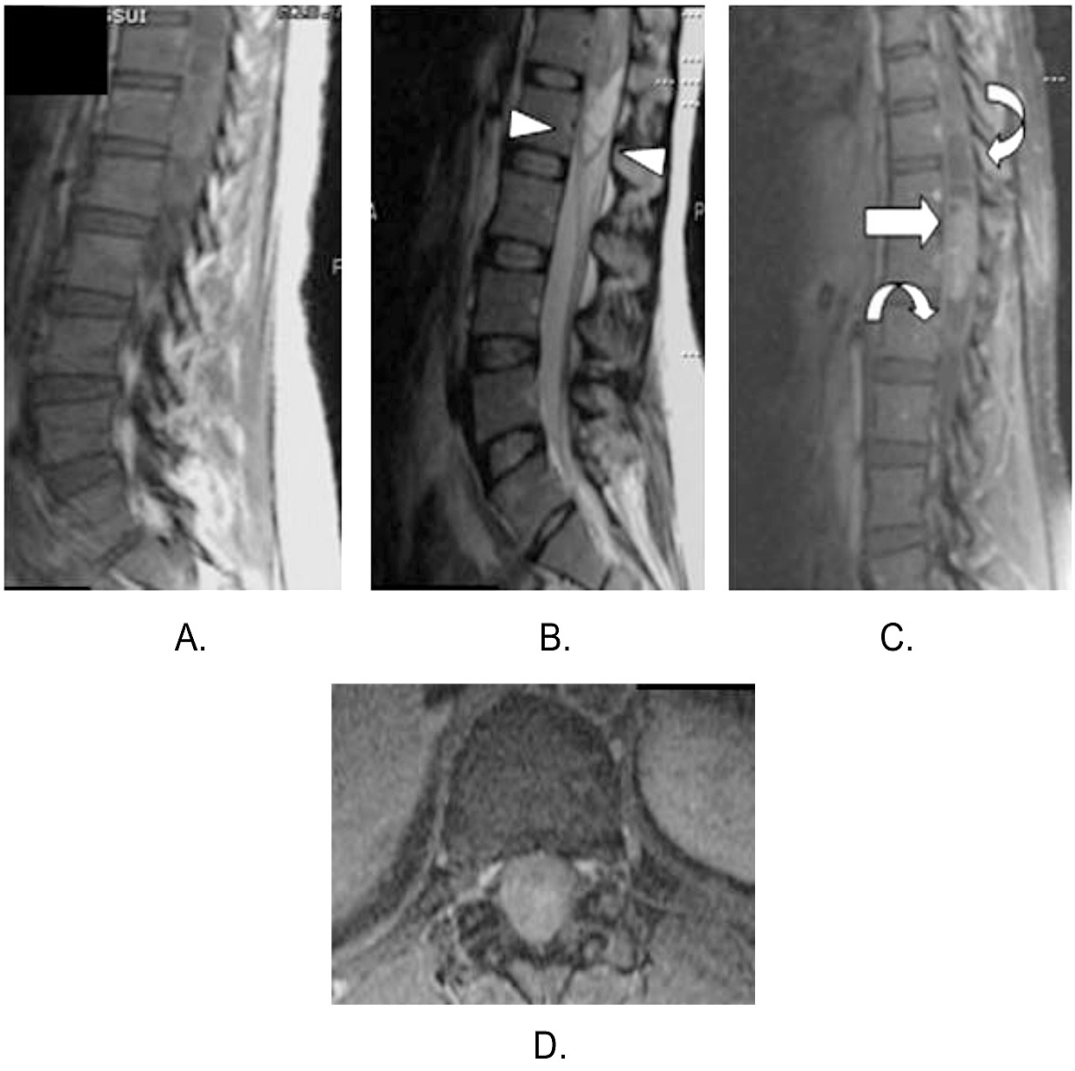

Fig 3 Spinal cord tanocytic ependymoma with rostral and caudal cysts (WHO grade II) in 36 year-old woman. (A) T1-weight sagittal image show heterogeneous iso-hypo signal intensity at conus medullaris region and exhibit hyper SI on (B) T2-weight sagittal image with peritumoral low SI (arrow head), representing hemosiderin cap sign. (C) and (D) Fat suppressed CE T1-weight sagittal and axial image show intense enhancement (white arrow) with rostral and caudal cysts (curve arrow).

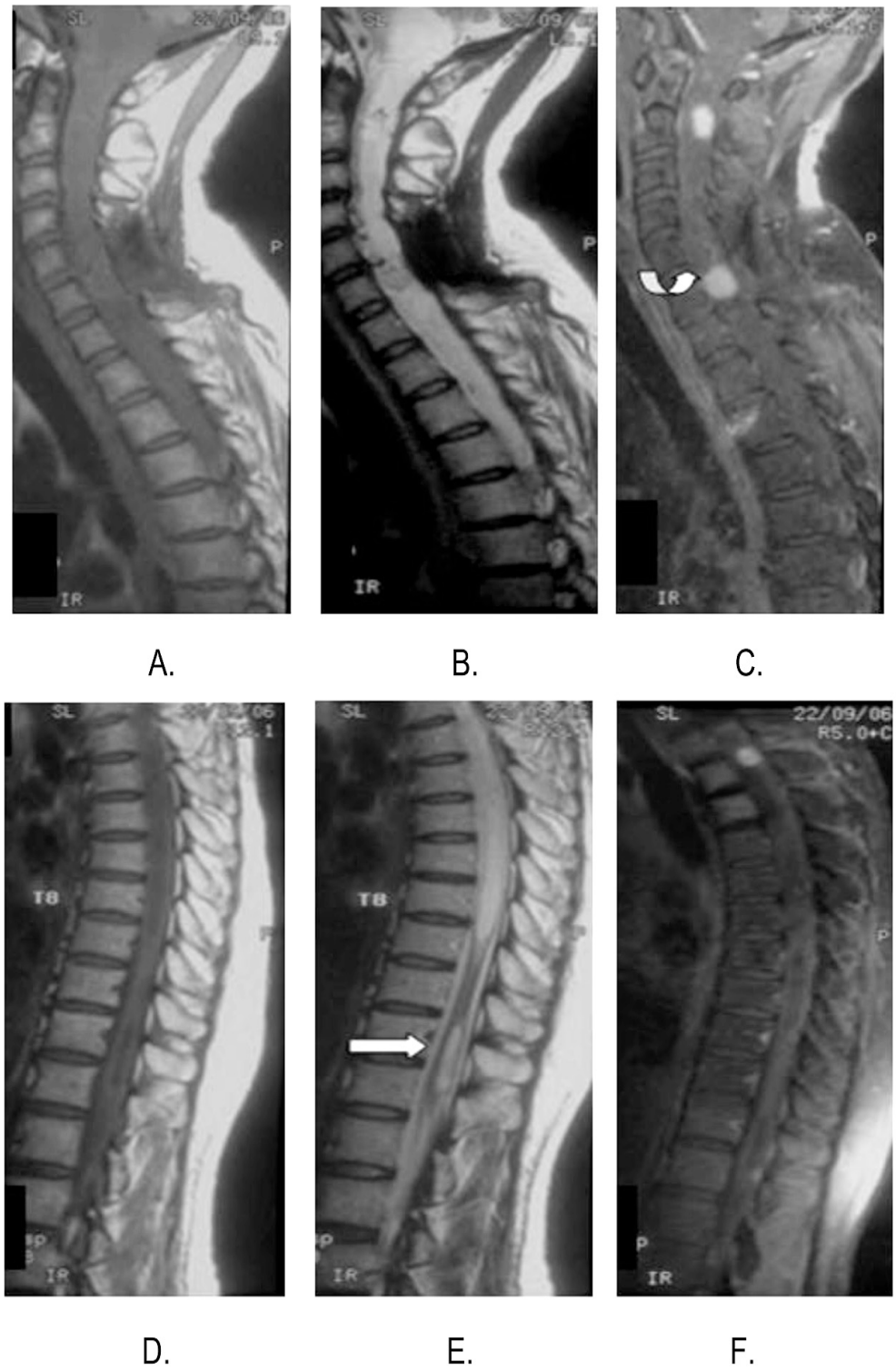

Fig 4 Spinal cord ependymoma with syringohydromyelia (WHO grade II) in 39 year-old woman. (A) T1-weight sagittal image show low signal intensity intramedullary tumors form C2-T12 spine and exhibit high signal intensity in (B) T2-weighted image. (C) Fat-suppressed CE T1-weighted sagittal image show patchy enhancement of intramedullary spinal cord lesions (curved arrow). (D) T1-weighted sagittal image (E) T2-weighted sagittal image and (F) Fat-suppressed CE T1-weighted sagittal image show intramedullary tumors extending to the thoracic spine with syringohydromyelia at T11/12 spine (white arrow).

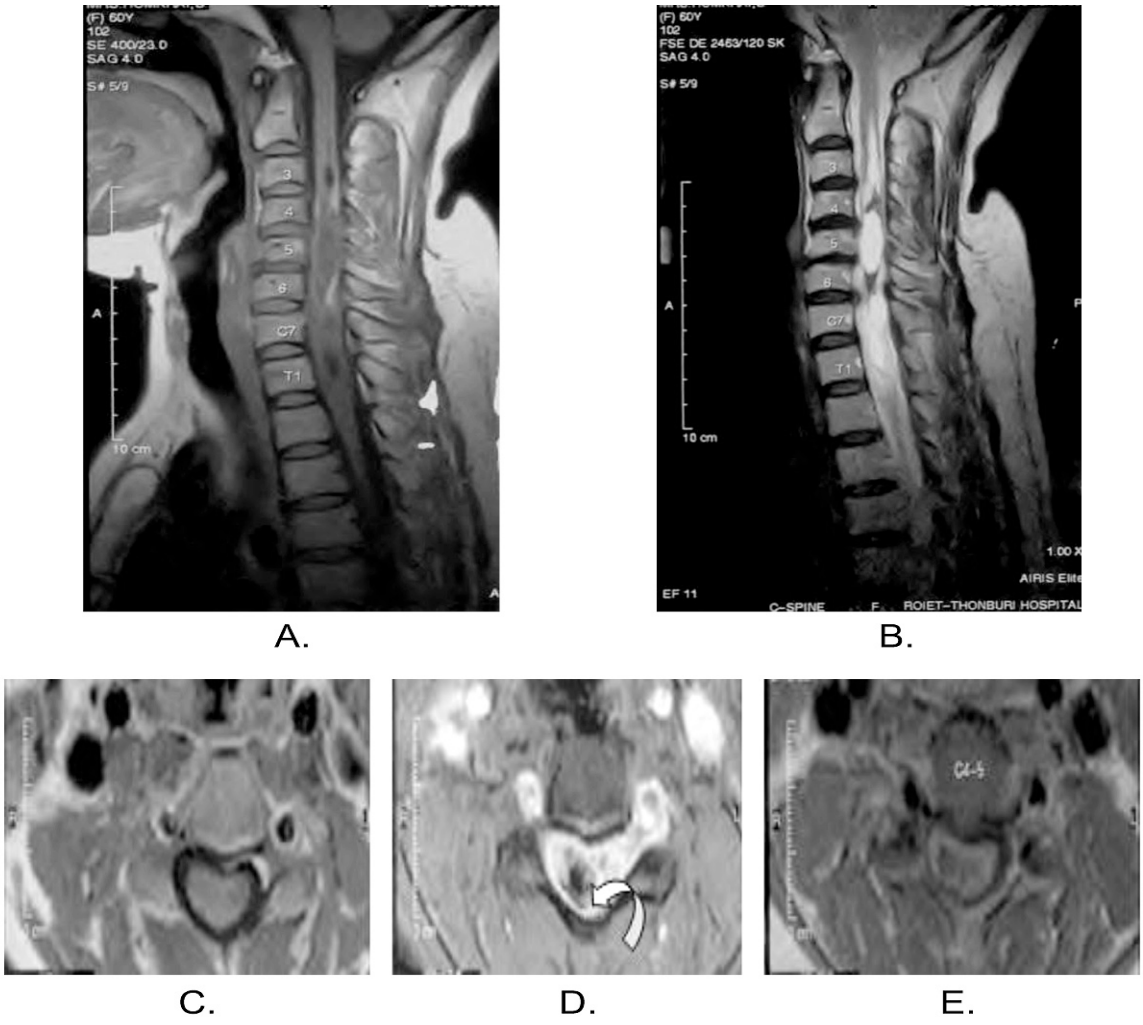

Fig 5 Spinal cord ependymoma with intratumoral hemorrhage (WHO grade II) in 60 year-old woman. (A) T1-weight sagittal image show well-defined mix iso-hyper SI intramedullary tumor from C3-T1 spine and exhibit hyper SI on (B) T2-weight sagittal image (arrow head). (C) T1-weight axial image show small area of hyper SI and exhibits low SI area with blooming artifact on (D) T2-weight gradient axial image, representing intratumoral hemorrhage (curved arrow). (E) Fat suppressed CE T1-weight axial image show heterogeneous enhancement pattern.

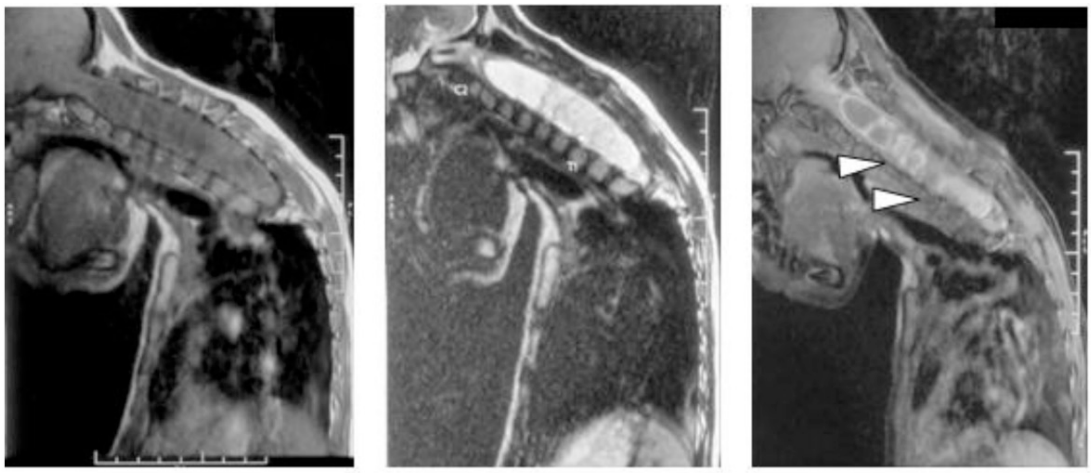

A. B. C.

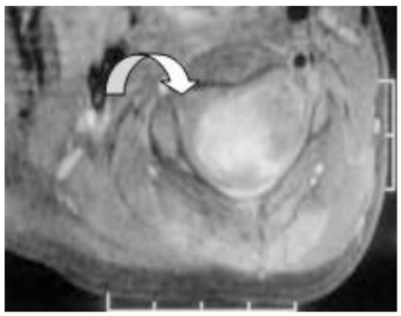

D.

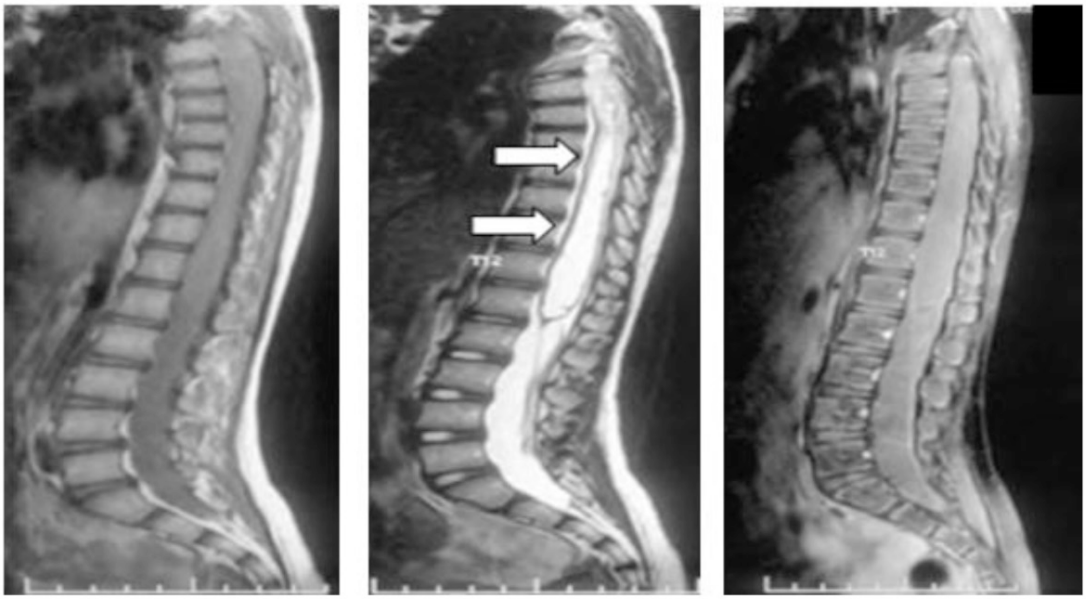

E. F. G.

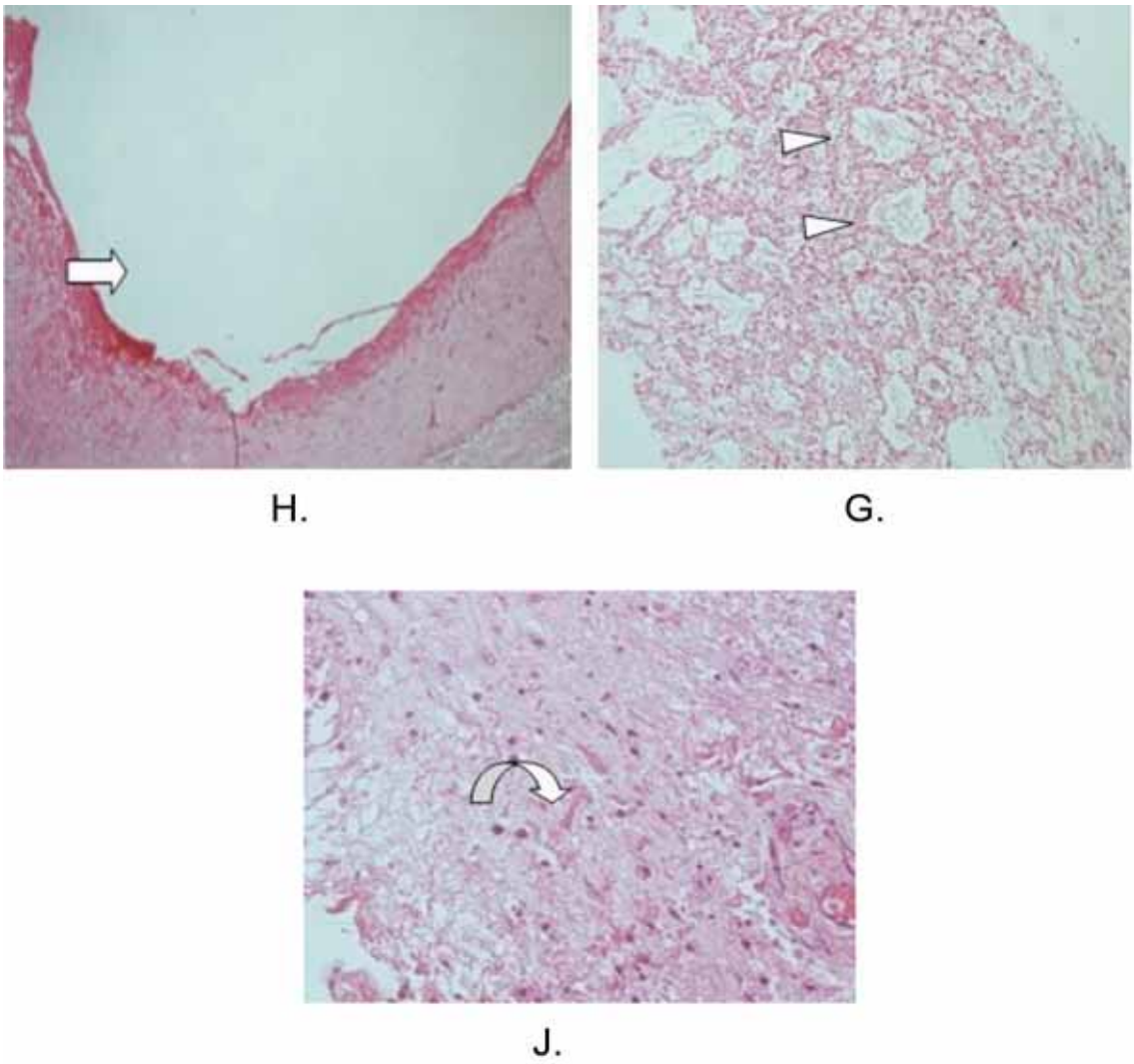

Fig 6 Spinal cord pilocytic astrocytoma (WHO grade I) in 9 years old girl presenting with scoliosis. (A) T1-weight sagittal image (TR/TE=700/12.5) show ill-define iso SI intramedullary spinal cord tumor form C2-T1 and exhibit heterogeneous hyper SI on (B) T2-weight sagittal image. (C) and (D) Fat suppressed CE T1-weight sagittal and axial image show heterogeneous enhancement of tumors (arrow head and curve arrow). (E) T1-weight sagittal image shows long segment of syringohydromyelia entire thoracic extending to lower lumbar spine and exhibit hyper SI on (F.) T2-weight sagittal image (white arrow). (G) Fat suppressed CE T1-weight sagittal image shows no enhancement of this lesions. (H), (I) and (J) Histology show a large cystic area (arrow), microcystic area (arrow head) and rosenthal fiber (curve arrow).

ependymomas are hypointense[8]. These tumors are sometimes heterogeneous due to hemorrhage. Sometimes dark caps were seen, especially on T2WI, rostral and caudal of the tumor representing hemosiderin deposits. Cyst formation and hemorrhage is common, especially at the tumor margins. Hemorrhage and calcification are more common than in astrocytomas[10]. After contrast administration intense enhancement is the rule, sometimes homogeneous, but often also heterogeneous of rim-like[8]. Most astrocytomas were iso- or hypointense relative to the spinal cord on T1-weighted imaging and hyperintense on T2-weighted imaging[2,8]. The enhancement patterns of the intramedullary astrocytomas, were evenly distributed with focal nodular, patchy, and inhomogeneous diffuse enhancement; however, non demonstrated a homogeneously diffuse enhancing pattern[2]. These patchy or irregular enhancements are one of the MR imaging characteristics of astrocytomas, differentiating them from ependymoma and are supposedly the result of the pathologic features of astrocytomas that tend to have an infiltrative nature extending far beyond the gross tumor margin. Therefore, patients with astrocytomas have a worse prognosis and survival rate than those with ependymomas.

At T2 imaging, the presence of a low-signal rim along the rostral or caudal margin of a spinal cord tumor is a fairly specific indicator of ependymoma, and was found in 17%, 20%, 20% and 64% of cases in the series investigated, respectively, by Choi et al.[11], Fine et al.[12], Alice et al.[13], and Nemoto et al[14]. The rim is due to the presence of hemosiderin at the margin of the tumor, arising, presumably, from prior subclinical tumoral hemorrhage, and is often referred to as a 'hemosiderin cap'. In our series was found only 1/8 (12.5%) of spinal cord ependymoma.

In the next category, the published literature states that 50% of spinal ependymomas will demonstrate associated cysts[7]. There are two basic types of cysts: tumoral and nontumoral. Cysts located at the poles of the solid portion of the tumor usually represent simply reactive dilatation of the central canal (syringomyelia). Approximately 60% of all intramedullary spinal tumors demonstrate these rostral or caudal[15]. In these cases, only the solid component of a spinal cord tumor must be resected; the rostral and caudal cysts will either decompress upon removal of the solid portion or they can be aspirated by the surgeon at resection[7,15]. In fact, rostral and caudal cysts have been shown to contain either hemorrhagic or xanthochromic fluid, but never tumor cells[7]. These cysts are not part of the tumor itself and should not enhance on imaging studies. They are not septated and do not show echogenicity within their walls at intraoperative ultrasonography (US)[15]. Rostral or caudal cysts are believed to arise from the egress of fluid produced by these neoplasms through the central canal and may also explain the relative lack of symptoms seen in cases of intramedullary spinal neoplasms. In contrast, tumoral cysts are contained within the tumor itself and frequently show peripheral enhancement[7,15]. They tend to be more commonly seen in astrocytomas than in ependymomas[15]. Identification of the location of the solid enhancing portion of the tumor (including enhancing tumoral cysts) is vital because current neurosurgical techniques allow laminotomy or laminectomy to be limited only to this zone, thereby decreasing potential surgical morbidity[7,15]. Balériaux et al, intratumoral cysts appeared in 4 astrocytomas (21%) and peritumoral cysts appeared in 3 (16%) patients[9]. In our series, patho-

logical findings show cystic component 57.1% of seven spinal cord astrocytomas and 37.5% of eight spinal cord ependymomas. Whereas MRI findings show rostal or caudal reactive cyst 87.5% of spinal cord ependymomas more common than spinal cord astrocytomas 28.6%.

Histological findings

Most ependymomas are histologically benign and well demarcated and compress the adjacent cord rather than infiltrating it. WHO grade is one component of a combination of criteria used to predict a response to therapy and outcome[16]. There are four histologic subtypes of ependymomas: cellular, papillary, clear cell, and tanocytic. The cellular form is the most common intramedullary variant. On histologic evaluation, perivascular pseudorosettes are the cardinal histologic feature (Fig 1), and there is moderate cellularity with low mitotic activity. The most common histologic subtypes are pilocytic astrocytomas (World Health Organization [WHO] grade I) and fibrillary astrocytomas (WHO grade II). Glioblastoma (WHO grade IV) rarely occurs in the spine, accounting for only 0.2-1.5% of cord astrocytomas. On histologic evaluation, fibrillary astrocytomas show widespread parenchymal infiltration with variable degrees of nuclear atypia and increased cellularity. Histologically, they are often biphasic with dense and looser areas. Pilocytic astrocytomas generally lack mitotic figures and other high-grade features and may harbor Rosenthal fibers (intracytoplasmic proteinaceous inclusions) (Fig 4) and thickened vascular walls. We found that in every cases ependymomas were mark hypervascularity, while 2/7 (28.2%) of astrocytoma were moderate hypervascularity. Therefore spinal cord ependymomas show homogeneous intense enhancement, but astrocytomas never. In our series, we found homogeneous enhancement of spinal cord ependymoms 1/8 (12.5%). Most of spinal cord ependymomas had cystic and hemorrhage component, possibly other enhancement patterns such as focal nodular, heterogeneous or patchy enhancement. Spinal cord astrocytomas show heterogeneous enhancement 4/7 (57.2%). Two of 15 cases (13.3%) were misinterpreted, the fist one of spinal cord ependymoma at cervical spine and the last one of hemorrhagic astrocytoma.

In our study, there are some limitations as following. The sample size was too small. The MRI was interpreted by one experienced neurological radiologist without intraobserver variability assessment. MRI gradient sequence was not performed in all cases which may lower sensitivity to detected intratumoral hemorrhage.

Conclusion

The correct diagnostic spinal cord tumor is important because the treatment and prognosis are different. MRI has significantly changed the detection and diagnosis of intramedullary spinal cord tumors. Although no statistically significant characteristic MRI feature to distinguish between ependymoma and astrocytoma is detected. By percentage we found that border, length and signal intensity of tumors may help diagnosis. With pathological correlation, all of spinal cord ependymomas are mark hypervascular tumor, but astrocytomas never showed.

References

1. Sun, B., Wang, C., Wang, J. MRI features of intramedullary spinal cord ependymomas. Journal of Neuroimaging 2003;13(4):346-51.

2. H.S. Seo, J.-h. Kim, D.H. Lee. Nonenhancing Intramedullary Astrocytomas and Other MR Imaging Features: A Retrospective Study and Systematic Review. AJNR 2010; 31:498-503.
3. Kasim Abul-Kasim, Majda M. Thurnher. Intradural spinal tumors: current classification and MRI features. Neuroradiology 2008;50:301-14.
4. Lowe, G.M. Magnetic resonance imaging of intramedullary spinal cord tumors. Journal of Neuro-Oncology 2000; 47(3):195-210.
5. Fred J. Epstein, Jean-Pierre Farmer, F.R.C.S., and Diana Freed. Adult intramedullary astrocytomas of the spinal cord. J Neurosurg 1992;77:355-9.
6. John K. Houten and Paul R. Cooper. Spinal cord astrocytomas: presentation, management and outcome. Journal of Neuro-Oncology 2000;47:219-24.
7. Heather Kahan, Evelyn M. L. Sklar. MR Characteristics of Histopathologic Subtypes of Spinal Ependymoma. AJNR 1996;17:143-50.
8. J.W.M. Van Goethem et al. Spinal tumors. European Journal of Radiology 2004; 50:159-76.
9. Balériaux, D.L.F.Spinal cord tumors. European Radiology 1999;9(7):1252-8.
10. Bloomer, C.W., Ackerman, A., Bhatia, R.G. Imaging for spine tumors and new applications. Topics in Magnetic Resonance Imaging 2006;17(2):69-87.
11. Choi, J.-Y., Chang, K.-H. Intracranial. Spinal Ependymomas: Review of MR Images in 61 Patients. Korean Journal of Radiology 2002;3(4):219-28.
12. Fine MJ, Kricheff II, Freed D, Epstein FJ. Spinal cord ependymomas: MR imaging features. Radiology 1995; 197:655-8.
13. Alice Boyd Smith. Karl A. Soderlund. Radiologic-Pathologic Correlation of Pediatric and Adolescent Spinal Neoplasms. AJR 2012;198:34-43.
14. Nemoto Y, Inoue Y, Tashiro T, et al. Intramedullary spinal cord tumors: significance of associated hemorrhage at MR imaging. Radiology 1992;182:793-6.
15. Kelly K. Koeller, CDR, R. Scott Rosenblum. Neoplasms of the Spinal Cord and Filum Terminale: Radiologic-Pathologic Correlation. RadioGraphics 2000;20:1721-49.
16. Louis, D.N., Ohgaki, H. The 2007 WHO classification of tumours of the central nervous system. Acta Neuropathologica 2007;114(2):97-109.